

Visual mate preference evolution during butterfly speciation is linked to neural processing genes

Matteo Rossi^{1,2}, Alexander E. Hausmann¹, Timothy J. Thurman^{2,3}, Stephen H. Montgomery⁴, Riccardo Papa^{2,5,6}, Chris D. Jiggins⁷, W. Owen McMillan² & Richard M. Merrill^{1,2*}

1. Division of Evolutionary Biology, LMU, Munich, Germany; 2. Smithsonian Tropical Research Institute, Panama City, Panama; 3. Division of Biological Sciences, University of Montana, USA; 4. School of Biological Sciences, University of Bristol, Bristol, UK; 5. Department of Biology, University of Puerto Rico, San Juan, Puerto Rico; 6. Molecular Sciences and Research Center, University of Puerto Rico, San Juan, Puerto Rico; 7. Department of Zoology, University of Cambridge, Cambridge UK. *corresponding author: merrill@bio.lmu.de

Many animal species remain separate not because they fail to produce viable hybrids, but because they “choose” not to mate. However, we still know very little of the genetic mechanisms underlying changes in these mate preference behaviours. *Heliconius* butterflies display bright warning patterns, which they also use to recognize conspecifics. Here, we couple QTL for divergence in visual preference behaviours with population genomic and gene expression analyses of neural tissue (central brain, optic lobes and ommatidia) across development in two sympatric *Heliconius* species. Within a region containing 200 genes, we identify five genes that are strongly associated with divergent visual preferences. Three of these have previously been implicated in key components of neural signalling (specifically an *ionotropic glutamate receptor* and two *regucalcins*), and overall our candidates suggest shifts in behaviour involve changes in visual integration or processing. This would allow preference evolution without altering perception of the wider environment.

The evolution and maintenance of new animal species often relies on the emergence of divergent mating preferences^{1,2}. Changes in sensory perception or other neural systems must underlie differences in innate behaviours between species, and will ultimately have a genetic

31 basis. However, although the significance of behavioural barriers for speciation has been
32 recognized since the Modern Synthesis³, we know almost nothing of the genes underlying
33 changes in mating preferences, or variation in behaviours across natural populations more
34 broadly^{4,5}. Identifying these genes will provide an important route towards understanding how
35 behavioural differences are generated, both during development and across evolutionary time.

36 Previous studies of isolating preference behaviours have largely been limited to the
37 identification of causal genomic regions, which almost invariably contain many genes^{6,7,8,9}.
38 Only a handful of studies have identified likely candidate genes that contribute to species
39 behavioural preferences. These are largely limited to chemosensory-guided mating
40 preferences^{10,11,12,13}, and have identified changes at chemoreceptor genes. To our knowledge,
41 only two studies – in incipient fish species – have identified candidates for visual preference
42 evolution, albeit indirectly, both suggesting a role for sensory perception mediated by changes
43 in the peripheral visual system^{14,15}. Whether or not visual preference evolution generally
44 involves shifts at the sensory periphery, or in downstream processing, remains unknown.

45 The closely related species *Heliconius melpomene* and *H. cydno* differ in warning
46 patterns, which are both under disruptive selection for mimicry¹⁶ and are important mating
47 cues¹⁷. In central Panama, *H. melpomene* shares the black, red and yellow pattern of its local
48 *Heliconius erato* co-mimic. In contrast, *H. cydno* mimics the black and white patterns of *H.*
49 *sapho*. The two species remain separate largely due to strong assortative mating¹⁸. Visual
50 preferences for divergent patterns are particularly apparent in males, which strongly prefer to
51 court conspecific females^{17,19,20}. Differences in warning pattern between *melpomene* and
52 *cydno* are largely due to expression differences in just three genes, specifically *optix*²¹,
53 *WntA*²² and *cortex*²³.

54 Quantitative trait locus (QTL) mapping of *H. melpomene* and *H. cydno* has revealed
55 three genomic regions of major effect that influence the relative time males spend courting
56 red *melpomene* or white *cydno* females²⁰. Notably, the best supported QTL was in the same

57 genomic region as *optix*, the gene responsible for presence of the red colour pattern elements
58 in *H. melpomene*²¹. Genetic linkage will facilitate speciation by impeding the breakdown of
59 genetic associations between ecological and mating traits²⁴. Nevertheless, this QTL, and its
60 associated candidate region, contain hundreds of genes, and the exact genes responsible for
61 differences in preference behaviour are not known.

62 Here, we first confirm that the behavioural QTLs identified previously are associated
63 with variation in male courtship initiation. We then identify genes within the major QTL,
64 which were differentially expressed in the neural tissue (central brain, optic lobes and
65 ommatidia) of *H. melpomene* and *H. cydno*, or have protein coding changes predicted to alter
66 protein function. Out of 200 genes within the QTL region, we identify just five candidates
67 likely to underlie assortative mating behaviours.

68

69 **Results**

70 **Chromosome 18 is associated with differences in courtship initiation.**

71 Our previous results reveal that QTLs on chromosomes 1, 17 and 18 influence the relative
72 time hybrid males spend courting red *melpomene* or white *cydno* females²⁰. However, the
73 time males spend courting a particular female might depend not only on male attraction, but
74 on the female's response (and in turn his response to her behaviour). To confirm that these
75 previously reported QTLs influence male approach behaviours (as opposed to other traits that
76 may influence courtship, for example male morphology²⁵), we reanalysed our previous data,
77 this time explicitly considering whether males initiated courtship towards *melpomene*, *cydno*
78 or both types of female during choice trials. Consistent with our previous analyses²⁰, we
79 found that F1 and backcross-to-*melpomene* prefer to court *melpomene* females, whereas
80 courtship initiation behaviours segregate in the backcrosses to *cydno* (Figure 1). Notably,
81 backcrosses-to-*cydno* males heterozygous at the QTL on chromosome 18 (*i.e.* with a
82 *melpomene* allele derived from the F1 father) initiated courtship towards *melpomene* females

83 more frequently than males homozygous for the *cydno* allele (Figure 1, bottom left; $n = 139$,
84 ΔELPD : -10.9 (S.E. \pm 5.1), *i.e.* a change of 2.14 SE units). Together with previous evidence
85 that male hybrids bearing *melpomene* alleles at *optix* prefer to court the artificial models of
86 *melpomene* females over those of *cydno*²⁶, these results suggest that the QTL on chromosome
87 18 harbours genes for visual attraction behaviours towards females with the red pattern.
88 Consequently, we focused our subsequent analyses on this QTL on chromosome 18 (and also
89 because tight linkage of *optix* allowed us to track the alleles at preference-colour locus in
90 hybrid crosses). The QTL on chromosome 1 was also retained in our model of initiation
91 behaviours (Supplementary figure 1; $n = 139$, $\Delta\text{ELPD} = -13.6$ (SE \pm 5.7), *i.e.* a change of 2.34
92 SE units), in contrast to the QTL on chromosome 17 which was not retained ($n = 139$,
93 $\Delta\text{ELPD} = -2.1$ (S.E. \pm 3.0)). Results for the QTL on chromosome 1 are reported in the
94 supplementary materials (Supplementary table 1).

95

96 **27 genes within the major QTL are differentially expressed in the brains and eyes of *H.***
97 ***cydno* and *H. melpomene*.**

98 We hypothesized that changes in gene regulation that determine differences in visual mate
99 preference behaviours might occur during pupal development (for instance, during visual
100 circuit assembly) or in the imago, and must involve changes in the peripheral and/or central
101 nervous system²⁷. Therefore, we generated RNA-seq libraries for combined eye and brain
102 tissue, across two pupal stages (around the time of ommochrome pigment deposit and half-
103 way through pupal development) and one adult stage, for *H. melpomene* and *H. cydno* and
104 compared their gene expression levels. We found considerable differential expression at the
105 QTL on chromosome 18 (the QTL spans 2.75 Mb, and contains 200 genes). We identified 27
106 genes within the QTL region that show differential expression between *melpomene* and
107 *cydno*, in at least one of the three developmental stages. These were mostly located within the
108 QTL peak (*i.e.* the genomic region with strongest statistical association with male preference)

109 or in close proximity to *optix* (Figure 2). The same genes were frequently differentially
110 expressed across development (Supplementary table 1), with 11 genes being differentially
111 expressed in more than one stage.

112 The genomic region between the start of chromosome 18 and *optix* (comprising the
113 QTL peak) is highly divergent between *melpomene* and *cydno*²⁸, and divergent coding
114 sequences within this region could also introduce mapping biases of RNA-seq reads. To
115 account for this, we repeated the analysis having mapped to both the *H. melpomene* reference
116 genome²⁹ and to a *H. cydno* genome³⁰. Generally, we found similar patterns of differential
117 expression when mapping to the *H. cydno* genome (Supplementary figure 2, Supplementary
118 table 2). Nevertheless, in subsequent analyses we excluded two genes, HMEL034187g1 and
119 HMEL034229g1, which showed reversal of the fold change or did not show differential
120 expression when mapping to the *H. cydno* genome respectively.

121
122 ***A regucalcin and an ionotropic glutamate receptor are upregulated in both H. melpomene***
123 ***and F1 hybrid males.***

124 Our previous behavioural experiments suggest that the alleles for the *melpomene* behaviour
125 are dominant over the *cydno* alleles^{20,26} (Figure 1). Given this pattern of dominance, we
126 predicted that genes underlying variation in male preference to be up- or down- regulated in
127 the brains of both *melpomene* and first generation (F1) hybrid males, with respect to *cydno*.
128 Of the putative genes differentially expressed between *cydno* and *melpomene* reported above,
129 only four, within the QTL candidate region, were differentially expressed between the F1
130 hybrids and *cydno* (Figure 2). These included two *regucalcins* (also called *senescence marker*
131 *proteins-30*: HMEL013552g1, HMEL034199g1), an *ionotropic glutamate receptor*
132 (HMEL009992g4), which is a putative ortholog of *Grik2*, and one gene with no annotated
133 function (HMEL009992g1). We obtained the same results regardless of whether we
134 considered both males and females together, or males alone. Further inspection of spliced

135 mRNA-reads indicated that the two annotated *regucalcins* were in fact a single gene (from
136 now on referred to as *regucalcin2*). This was also the case for the *ionotropic glutamate*
137 *receptor* and the gene with no annotated function (from now on referred to as *Grik2*).

138

139 **Differential expression of *Grik2* in adults is likely due to cis-regulatory effects.**

140 To determine whether differences in gene expression levels between parental species were
141 due to *cis*- or *trans*-regulatory changes, we conducted allele specific expression (ASE)
142 analyses in adult F1 hybrids. In F1 hybrids, both parental alleles are exposed to the same
143 *trans*-environment, and consequently *trans*-acting factors will act on alleles derived from each
144 species equally (unless there is a change in the *cis*-regulatory regions of the respective
145 alleles). Therefore, differences in allele specific expression indicate changes in *cis*-regulatory
146 regions³¹. Both candidate genes (*Grik2* and *regucalcin2*) had a very low number of SNPs that
147 could differentiate the *melpomene* and *cydno* allele (using both gene models of the Hmel2.5
148 annotation and RABT annotation) and few reads mapped to these SNPs. Nevertheless, for
149 *Grik2*, the *melpomene* allele was significantly more highly expressed relative to the *cydno*
150 allele ($p=0.017$, Wald test), suggesting *cis*-regulatory effects (Figure 3). For *regucalcin2*,
151 although there was a tendency towards up-regulation of the *melpomene* allele, consistent with
152 *cis*-regulation, we did not have sufficient power-to rule out *trans*-only regulatory effects
153 (Figure 3; $p=0.108$, Wald test).

154

155 ***Grik2* is differentially expressed in hybrids that essentially differ only for allelic**
156 **composition at the behavioural QTL region.**

157 In order to study the specific effects that *melpomene* derived alleles at the QTL on
158 chromosome 18 had on gene-expression, we introgressed this region into a *cydno* background
159 through multiple backcrosses (crossing design in Supplementary figure 3). We wanted to
160 investigate whether differences at this QTL regulated expression of any specific genetic

161 pathway during development, and more generally what changes in genome-wide transcription
162 were observed in hybrids differing (mostly) just at this QTL region.

163 Notably, in these third-generation backcross hybrid comparisons, across the entire
164 genome only 23 and 29 genes were differentially expressed (at 156h after pupal formation
165 (APF) and at 60hAPF, respectively). Of these, 20 and 19 genes (at 156hAPF and at 60hAPF,
166 respectively) were located on chromosome 18, indicating that gene expression differences in
167 these comparisons were mostly restricted to the preference-colour region on chromosome 18,
168 segregating for *cyd/melp* or *cyd/cyd* alleles. No genetic pathway was enriched for gene
169 expression differences between these hybrids at either pupal stage (PANTHER enrichment
170 test³²), suggesting that overall this QTL harbours a few, modular changes in gene regulation
171 in the developing brain/eyes of *cydno* and *melpomene*. *Grik2* was the only gene detected as
172 differentially expressed between species and hybrids at these pupal stages (Supplementary
173 figure 4).

174 To verify that differential expression of candidate genes at the QTL region is driven
175 by *melpomene* alleles on chromosome 18 and not by other *melpomene* alleles at *trans*-acting
176 genes on other chromosomes, we compared gene expression levels between hybrids carrying
177 *cyd/melp* vs. *cyd/cyd* regions on chromosomes chr1, chr4 and chr15, chr20 (Supplementary
178 figure 5A). In these comparisons, there was no signal of differential expression on
179 chromosome 18. This supports the *cis*-regulatory activity of the *melpomene* allele of
180 candidate genes on chromosome 18. To test this further, we conducted another allele specific
181 expression study in the BC3 hybrids, which suggested *trans*-regulatory effects for *Grik2* at
182 these pupal stages, but were less conclusive with regard to *regucalcin2* (Supplementary figure
183 6). Since causal gene/s might exert an effect on behaviour due to their action during
184 development or in adult form, and this action might in turn be differently (*cis*- vs *trans*-)
185 regulated, we still considered both genes as strong candidates.

186

187 **4 genes with protein-coding substitutions within the QTL candidate region have**
188 **predicted effects on protein function.**

189 Because shifts in behavioural phenotypes could be due to changes in protein-coding regions,
190 we additionally considered protein-coding substitutions between *melpomene* and *cydno*.
191 Overall, we found 152 protein-coding substitutions, spanning 54 of the 200 genes across the
192 entire QTL candidate region. We then studied whether these variants were predicted to have
193 non-neutral effects on protein function with PROVEAN³³. The PROVEAN algorithm predicts
194 the functional effect of protein sequence variations based on how they affect alignments to
195 different homologous protein sequences. We found 4 genes with such predicted effects
196 (PROVEAN score < -2.5): Specifically, a *WD40*-repeat domain containing protein
197 (HMEL013551g3), a *cysteine protease* (HMEL009684g2), a *MORN* motif containing protein
198 (HMEL006660g1), and another *regucalcin* (HMEL013551g4) adjacent to, but distinct from,
199 that found to be differentially expressed above (from now on referred to as *regucalcin1*).

200

201 **Candidate genes occur in regions with reduced gene flow.**

202 Of our six candidate genes for preference behaviours that contribute to reproductive isolation
203 between *H. cydno* and *H. melpomene* (*regucalcin2*, *Grik2* and the four genes with protein
204 coding modifications), five are found within the QTL peak (Figure 4). Genetic changes
205 causing reproductive isolation between populations are expected to reduce localized gene
206 flow in their genomes. Therefore, we compared the position of our candidate genes to
207 estimated levels of admixture proportions (f_d)³⁴ between *H. melpomene* and *H. cydno* across
208 the QTL candidate region³⁵. We found that all candidate genes were located in genomic
209 regions with low f_d values (Figure 4), suggesting localized resistance to gene flow between
210 *melpomene* and *cydno* at these genes and their putative *cis*-regulatory regions.

211

212

213 Discussion

214 Behavioural isolation is frequently implicated in the formation of new species, and involves
215 the correlated evolution of both mating cues and mating preference. Here we have analysed a
216 genomic region in a pair of closely related sympatric butterflies, *H. cydno* and *H. melpomene*,
217 that contains genes for divergence in both an ecologically relevant mating cue and the
218 corresponding preference. Physical linkage between ecological and mating traits will facilitate
219 speciation by allowing different barriers to act in concert to restrict gene flow^{36,37}. Although
220 the genes underlying changes in the warning pattern cue in *Heliconius* are well
221 characterized^{21,22,23,38} (e.g. *optix*), those underlying the corresponding shift in behaviour have
222 not previously been identified^{20,39,40}. We have pinpointed a small number of genes that fall
223 within the QTL peak, which show either expression (*regucalcin2* and *Grik2*) or protein
224 coding differences (HMEL013551g3, HMEL009684g2, HMEL006660g1, and *regucalcin1*)
225 and fall within a region of reduced admixture, that are strong candidates for modulating
226 mating behaviour.

227 Two broad neural mechanisms could underlie the evolution of divergent visual
228 preferences, involving changes in either i) detection at the sensory periphery or ii) the
229 processing and/or integration of visual information. Although *H. melpomene* and *H. cydno*
230 have the same retinal mosaics/class of photoreceptors⁴¹, spectral sensitivity in the *Heliconius*
231 eyes could be altered by filtering pigments⁴², or other physiological processes taking place at
232 the photoreceptors/sensory periphery, eventually shifting sensitivity towards different
233 wavelengths (and possibly colour patterns). It has previously been hypothesized that the gene
234 regulatory networks for ommochrome deposition in the *Heliconius* eyes might have been co-
235 opted in the wings⁴³, where *optix* plays a central role, and therefore that *optix* might play a
236 role in eye pigmentation in *Heliconius*. However, the protein product of *optix* has not been
237 detected in pupal or adult retinas of various *Heliconius* species tested⁴⁴, and therefore has no
238 obvious link to ommochrome deposition in the eyes. More generally, the underlying

239 evolutionary mechanism is unlikely to involve detection at photoreceptors, as this would
240 probably have a broad effect on downstream processing² and alter the visual perception of the
241 animal's wider environment.

242 The second mechanism, involving changes in the processing, and/or integration, of
243 visual information, could act through an alteration of neuronal activity or connectivity. For
244 instance, different levels of gene expression in conserved neural circuits between *melpomene*
245 and *cydno* may affect overall synaptic weighting and determine whether a signal (e.g. colour
246 and motion) elicits a motor pattern (response towards a female) or not. Consistent with this
247 scenario, the composition of ionotropic receptors at post-synapses is a key modulator of
248 synaptic transmission⁴⁵, implicating *Grik2*. Interestingly, differential expression of ionotropic
249 glutamate receptors is also associated with variation in social and aggressive behaviours in
250 vertebrates^{46,47}. *Regucalcins* are involved in calcium signalling⁴⁸, which regulates synaptic
251 excitability and plasticity⁴⁹, and has an important role in axon guidance⁵⁰ (albeit alongside
252 additional roles across a broad range of biological processes), making the two *regucalcins* we
253 identify strong candidates for behaviour.

254 Changes in the regulation of genes with pleiotropic effects are likely to be less
255 detrimental compared to changes in their protein-coding sequences⁵¹ (although emerging
256 evidence has begun to suggest that enhancer/repressor elements may be more pleiotropic than
257 previously thought^{52,53}). Furthermore, there is considerable evolutionary potential in the co-
258 option of transcription factors/networks⁵¹ that regulate neural patterning or neuron-type
259 activity, possibly resulting in novel adaptive expression patterns. In line with this,
260 *Regucalcin2* and *Grik2*, which are differentially expressed in the eyes and brain in both our
261 species and hybrid comparisons, are likely to be involved in multi-functional processes, such
262 as calcium signalling and ion transport, and likely have pleiotropic alleles. We also found
263 evidence of cis-regulatory effects for both genes (albeit not significant for *regucalcin2*),

264 which would be required of the causal genetic change within the QTL, if it were to be in gene
265 regulation.

266 Despite expectations that non-coding, regulatory loci may provide a flexible route to
267 divergent mating preferences, we also found substitutions in coding regions at the QTL,
268 which are predicted to have an effect on protein functioning and therefore remain strong
269 candidates. These genes include *regucalcin1*, which is distinct from, but located next to,
270 *regucalcin2* (which is differentially expressed). Notably, the eye transcript of *regucalcin1* was
271 recently characterized as fast-evolving across *Heliconius* species⁵⁴. Other candidates include a
272 *cysteine protease*, which functions in protein degradation, and might be linked to behaviour
273 for example through degradation of neurotransmitters, a *MORN* motif containing protein
274 (function unknown), and a *WD40* containing protein. *WD-repeat* containing proteins have
275 been implicated in a wide array of functions ranging from signal transduction to apoptosis
276 (<https://www.ebi.ac.uk/interpro>).

277 Although preference for red colouration and the *optix* gene are tightly linked, we find
278 no evidence that *optix* is differentially expressed in the eyes or brains of our two species. It is
279 also not located within the QTL peak (and it contains no non-synonymous changes in protein
280 coding regions²¹). It seems unlikely therefore that changes in cue and preference are
281 pleiotropic effects of the same allele. More generally, although we have pinpointed the
282 strongest candidates yet identified for assortative mating behaviours in *Heliconius*, it is
283 possible that actual causal changes in gene regulation are restricted to developmental stages
284 other than those sampled, or restricted to a few neuronal populations not detected with
285 transcriptomic data from eyes and whole brain tissue. Nonetheless, by sampling at two pupal
286 stages (around the time of *optix* expression/ommochrome pigment deposit in the wing/eye and
287 halfway through pupal development) and at the adult stage, we should have captured
288 important transitions for the behavioural programming of the two species.

289 Work in the past decade has shown that complex innate behavioural differences
290 between species can be encoded in relatively few genetic modules^{55,56}, but very few
291 studies^{57,58,59} have identified specific genes underlying behavioural evolution. In particular,
292 traditional laboratory organisms continue to provide important insights into the evolution and
293 genetics of behaviour^{27,58,60}, however, comparative approaches are required to determine if
294 developmental principles can be broadly applied, and also to incorporate a wider range of
295 phenotypic variation and sensory modalities. The challenge now is to increase the resolution
296 of studies in non-traditional systems, in order to link individual genetic elements to
297 behaviours, *and* the sensory and/or neurological structures through which they are mediated.
298 In this light, we have identified a small handful of strong candidate genes associated with the
299 evolution of visual mate preference behaviours in *Heliconius*. These genes are in tight
300 physical linkage with the locus for the corresponding shifts in an ecologically relevant mating
301 cue, providing an important opportunity to investigate the build-up of genetic barriers crucial
302 to speciation. The candidate genes identified seem more likely to alter visual processing or
303 integration, rather than detection at photoreceptors, consistent with permitting changes in
304 mate preference without altering perception of the animal's wider environment.

305

306 **Materials and Methods**

307 **Courtship initiation analyses.** Butterfly rearing, crossing design and genotyping are
308 described in detail elsewhere²⁰. In brief, we assayed male preference behaviours for *H.*
309 *melpomene*, *H. cydno*, their first generation (F1) hybrids and backcross to hybrids to both
310 parental species in standardized choice trials. Males were introduced into outdoor
311 experimental cages (1x1x2m) with a virgin female of each species and courtship behaviours
312 recorded. Whenever possible, trials were repeated for each male (median = 5 trials). To
313 determine whether previously identified QTLs for courtship time contribute to variation in
314 courtship *initiation* behaviours, we performed a *post-hoc* analysis using categorical models in

315 a Bayesian framework with a multinomial error structure, using the R package *brms*. All
316 models were run under default priors (non- or very weakly informative). In contrast to our
317 previous analysis²⁰, in which we considered the number of minutes (*i.e.* time) for which
318 courtship was directed towards *H. cydno* or *H. melpomene* females, here the response variable
319 was number of trials in which male courtship was *initiated* towards *H. cydno* females only, *H.*
320 *melpomene* females only, or both female types (hereafter referred to as “*initiation*”). Across
321 males the median number of trials with a response was 3. Using backcross-to-*cydno* males
322 only, we fitted *initiation* as a response variable to genotype (*cyd/cyd* or *cyd/melp*) at each
323 QTL, which were included as separate fixed effects. Individual ID was fitted as random
324 factor. To test the effect of each QTL on male *initiation*, we compared the saturated model
325 incorporating all three QTL with reduced models excluding each QTL in turn, using
326 approximate leave-one-out (LOO) cross-validation⁶¹ as implemented in *brms*, and based on
327 expected log pointwise predictive density (ELPD). Normal distribution of ELPD can be a
328 straightforward approximation given our large samples sizes (n=139)⁶¹. Therefore, we
329 considered an absolute value of ELPD greater than 1.96 units of its standard error as
330 indicative of the reduced model being less-informative than the saturated model (95%
331 confidence). Males that did not initiate courtship to any female across trials were excluded
332 from analyses, resulting in a dataset of 139 males, from a total of 146 backcross males for
333 which we had genotype data. Finally, we extracted predictors and credibility intervals for
334 backcross males with differing genotypes from the minimum adequate model. Credibility
335 intervals for *H. melpomene*, *H. cydno*, F1 hybrid and backcross to *melpomene* males
336 displayed in Figure 1 were generated following the same procedures. Raw data and analysis
337 code are available in the following github repository:
338 https://github.com/SpeciationBehaviour/neural_genes_heliconius.git

339 **Butterfly collection, rearing and crossing design for expression analyses.** Wild *H.*
340 *melpomene rosina* and *H. cydno chioneus* individuals were caught along Pipeline Road near
341 Gamboa, Panama, in the Soberania National Park, and used to establish stocks at the
342 Smithsonian Tropical Research Institute insectaries in Gamboa. Butterflies were reared in
343 common garden conditions, in 2x2x2m cages, and provided with fresh *Psiguria* flowers and
344 10% sugar solution. Larvae were reared on fresh *Passiflora* shoots/leaves until pupation. *H.*
345 *cydno*, *H. melpomene* and hybrid individuals used for RNA-seq (see below) were reared
346 concurrently and under the same conditions. F1 hybrids were obtained by crossing a wild-
347 caught *H. m. rosina* male to an insectary-bred virgin *H. c. chioneus* female.

348 The introgression line was generated by outcrossing a hybrid male with a red forewing
349 band (crossing design shown in Supplementary figure 3) to virgin *H. cydno* females, over
350 three generations. The peak of the behavioural QTL reported previously²⁰ on chromosome 18
351 (at 0cM) is in very tight linkage with the *optix* colour pattern locus (at 1.2cM), which controls
352 for the presence and absence of the red forewing band seen in *H. melpomene rosina*. Presence
353 of the red forewing band is dominant over its absence so that segregation of the red band can
354 be used to infer genotype at the *optix* locus. Specifically, hybrid individuals with a red
355 forewing band are heterozygotes for *H. melpomene/H. cydno* alleles at the *optix* locus,
356 whereas individuals lacking the red band are homozygous for the *cydno* allele. Due to the
357 tight linkage we expected little recombination between *optix* and QTL peak even after three
358 generations of introgression, allowing us to infer genotype at the preference-*optix* locus
359 (which we confirmed with genetic data, see below).

360 **Tissue dissection, RNA extraction and mRNA sequencing.** Eye (ommatidia and retinal
361 membrane) and brain tissue (central brain and optic lobes) were dissected out of the head
362 capsule in cold (4 °C) 0.01M PBS solution, at two pupal stages: 60 hours after pupal
363 formation (60h APF) and 156h APF; and in adults aged 9 - 13 days. We sampled adults at

364 around 10 days of age because by this stage males are mature and frequently court females⁶².
365 Adult males and females sampled were sexually naive. We decided to sample at 60h APF
366 because this is the developmental stage at which *optix* is expressed in the wing, so we
367 hypothesized that it might had also been when *optix* is expressed in the brain. We sampled at
368 156h APF as a putative stage halfway through pupal development, and at this stage most of
369 the major neural connections have just been established in the *Heliconius* brain (Stephen
370 Montgomery, unpublished data).

371 Tissues were stored in RNAlater at 4 °C for 24 hours, and subsequently at -20 °C, until
372 RNA extraction. Total RNA was extracted using TRIzol Reagent (Thermo Fisher, Waltham,
373 MA, USA) and a RNeasy Mini kit (Qiagen, Valencia, CA, USA). Samples were treated with
374 DNase I (Ambion, Darmstadt, Germany). Integrity of total RNA was checked either on an
375 agarose gel or using an Agilent Bioanalyzer 2100 (Agilent Technologies, Santa Clara, CA,
376 USA). RNA concentration was measured on a Nanodrop spectrophotometer. Illumina TruSeq
377 RNA-seq libraries were prepared and sequenced at Edinburgh Genomics (Edinburgh, UK)
378 with 100 bp paired-end reads. To avoid lane effects the distribution of the species samples
379 was randomized on the sequencing platform. More detailed information about individuals and
380 sequencing yields can be found in the Supplementary dataset.

381
382 **RNA-seq read mapping and differential gene expression analyses.** After a quality control
383 of RNA-seq reads with FastQC, we trimmed adaptor and low-quality bases using TrimGalore
384 v.0.4.4 (<https://www.bioinformatics.babraham.ac.uk/projects/>). RNA-seq reads were mapped
385 to the *H. melpomene* 2.5 genome²⁹/annotation⁶³ using STAR v.2.4.2a⁶⁴ in 2-pass mode. We
386 only kept reads that mapped in ‘proper pairs’ using Samtools⁶⁵. The number of reads mapping
387 to each gene were estimated with HTseq v. 0.9.1⁶⁶ with model “union”, thus excluding
388 ambiguously mapped reads. Differential gene expression analyses between species/hybrids
389 were conducted in DESeq2⁶⁷. We considered only those genes showing a 2-fold change in

390 expression level, and at adjusted (false discovery rate 5%) p-values < 0.05, to be differentially
391 expressed, to exclude expression differences caused by known differences in brain
392 morphology⁶⁸ (Montgomery et al., in prep).

393
394 **Sexing pupae.** In all DESeq2 analyses, sex was included as a random factor. To sex pupae,
395 we first marked duplicate RNA mapped reads with Picard
396 (<https://broadinstitute.github.io/picard/>), and used GATK 3.8⁶⁹ to split uniquely mapped reads
397 into exon segments and trim sequences overhanging the intronic regions. We then used
398 Haplotype Caller on each individual, using calling and filtering parameters according to the
399 GATK Best Practices for variant calling on RNA-seq data. The sex of pupal samples was
400 inferred from the proportion of heterozygous (biallelic) SNPs using the R package SNPstats.
401 Males (ZZ) were expected to have >> 0% heterozygous sites, whereas females (ZW) to have
402 0%. Z-linked heterozygosity of the pupal samples (Supplementary table 3) were in line with
403 expectations (either ~ 0 for females or an order of magnitude higher for males), and matched
404 heterozygosity of either adult males or females, for which the sex was determined from
405 external morphology.

406
407 **Inference of gene function and transcript-based annotation.** Biological functions of
408 annotated genes were inferred with InterProScan v5⁷⁰, using the corresponding Hmel2.5
409 predicted protein sequences. InterProScan uses different databases like InterPro, Pfam,
410 PANTHER, and others, to infer functional protein domains and motifs (based on homology).
411 To study whether specific biological functions were enriched among genes showing
412 differential expression among hybrid types, we conducted the PANTHER enrichment test³⁸
413 (with Bonferroni correction for multiple testing) using *Drosophila melanogaster* as the
414 reference gene function database.

415 Upon detailed inspection of the mapping coverage of spliced RNA-seq reads to the
416 Hmel2.5 gene annotation, we noticed that some gene models were fragmented, namely, a few
417 exons that appeared to be spliced together were incorrectly considered distinct genes. To
418 check that this did not introduced inaccuracies in our differential gene expression analyses,
419 we re-annotated the *melpomene* genome using the Cufflinks reference annotation-based
420 transcript (RABT) assembly tool⁷¹ We used the transcriptomic data from both *melpomene* and
421 *cydno* to reannotate the *melpomene* genome, separately for every developmental stage, and
422 reconducted the differential gene expression analyses in DESeq2 as described above.
423 Repeating all comparative transcriptomic analyses using these new annotations (where exons
424 were correctly considered as part of single genes), we confirmed that both *regucalcin2* and
425 *Grik2* were differentially expressed in both species and hybrids comparisons.

426

427 **Inference of BC3 hybrids genome composition.** In order to perform comparative
428 transcriptomic analyses between third-generation backcross hybrids (BC3) segregating at the
429 QTL on chromosome 18 (crossing design in Supplementary figure 3), we first determined
430 which genomic regions in these hybrids were heterozygous (*cyd/melp*) or homozygous
431 (*cyd/cyd*). For this, we inferred variants from RNA-seq reads for each BC3 hybrid
432 (individually as above), and from the combined *melpomene* and *cydno* samples. For the
433 species, we used HaplotypeCaller⁶⁹ on RNA-seq samples from all developmental stages of
434 either species, to produce individual genomic records (gVCF), and then jointly genotyped
435 *melpomene* and *cydno* gVCFs (separately for the two species) using genotypeGVCFs with
436 default parameters. Genotype calls were filtered for quality by depth (QD) > 2, strand bias
437 (FS) < 30 and allele depth (DP) > 4. For further analyses we kept *biallelic* genotypes only.
438 We then used the *intersect* function of *bcftools*⁶⁵ to infer variants exclusive to the *cydno* and
439 to the *melpomene* samples.

440 We calculated the fraction of variants that each BC3 hybrid individual shared with the
441 *melpomene* and with the *cydno* samples, in non-overlapping 100kb windows. We compared
442 these to the fraction of variants that a F1 hybrid and a *H. cydno* individual (not included in the
443 combined genotyping of the *cydno* samples), shared with the same species samples, and found
444 that they matched either one of them, indicating heterozygous (*cyd/melp*) or homozygous
445 (*cyd/cyd*) regions (Supplementary figure 5B). In this analysis, we considered only those
446 100kb windows where BC3 hybrids/F1 hybrid/*H. cydno* individuals shared more than 30
447 variants with the *melpomene/cydno* samples.

448 To corroborate our findings, we repeated the same type of analysis, this time inferring
449 species-specific variants for *melpomene* and *cydno* using 10 *H. melpomene rosina* and 10 *H.*
450 *cydno chioneus* genome resequencing samples. Variant calling files (vcf) were retrieved from
451 Martin et al³⁵. We considered only *biallelic* genotype calls that had $10 < DP < 100$ and
452 genotype quality (GQ) > 30 . With this analysis we found the same heterozygous and
453 homozygous regions in BC3 hybrids.

454 The size and number of the introgressed regions were in line with expectations about
455 3rd generation backcross hybrids following our crossing design: segregating at the level of
456 chromosome 18 and at four other chromosomes. For the BC3 hybrids sampled at 156 hours
457 after pupal formation (APF) we had 6 *cyd/melp* and 10 *cyd/cyd* at the QTL region on
458 chromosome 18 (Supplementary figure 5A), for those at 60h APF, 8 *cyd/melp* and 9 *cyd/cyd*
459 hybrids at the same region.

460
461 **Allele-specific expression (ASE) in hybrids.** In order to conduct ASE analyses we first
462 identified species specific variants, fixed in either *melpomene* and *cydno*. For this, we took
463 the quality filtered variants inferred from the species genome resequencing data, and assigned
464 those genotype calls in *cydno* and *melpomene* for which allele frequency (AF) was > 0.9 as

465 homozygous (we did not consider indels in this analysis). We then used *bcftools intersect*⁶⁵ to
466 get only those variants for which *cydno* and *melpomene* had opposite alleles.

467 At the same time, we called variants from RNA-seq reads of F1 hybrid individuals,
468 again according to the GATK Best Practices (with the exception of parameters -window 35 -
469 cluster 3, to increase SNPs density), and selected only heterozygous SNPs in F1s that matched
470 the species-specific variants. Finally, we used GATK's ASEReadCounter⁶⁹, with default
471 parameters, to count RNA reads in the F1 hybrids (and later on in BC3 hybrids) that mapped
472 to either the *cydno* or the *melpomene* allele. We summed all reads mapping to either the *cydno*
473 or *melpomene* allele/variant within the same gene (both for gene models of the Hmel2.5 gene
474 annotation and for the Cufflinks annotation we assembled previously). To test for allele
475 specific expression (diffASE) we fitted the model “~0 + individual + allele” in DESeq2⁶⁷,
476 setting library size factors to 1 (thus not normalizing between samples, as the test for diffASE
477 is conducted within individuals). We only considered those alleles showing at least a 2-fold
478 change in expression and $p < 0.05$, as differentially expressed.

479 In order to check that there were no biases in alleles assignment to one of the two
480 species, we analyzed the ratios of the species alleles, for every gene, and checked that they
481 were not systematically biased to either one of the two species. The \log_2 fold-changes of the
482 species alleles were centered around 0, suggesting no obvious bias in alleles assignment⁷²
483 (Supplementary figure 7).

484

485 **Protein-coding substitutions and predicted effects on protein-function.** We inferred fixed
486 variants in protein-coding regions from the combined *melpomene* and *cydno* RNA samples in
487 order to include variants from genes for which we detected expression in the brain/eyes across
488 the 3 stages. We took the quality filtered variants called from the joint genotyping of RNA-
489 seq data of *cydno* and *melpomene* (from all stages), and selected those genotype calls for
490 which allele frequency (AF) > 0.8 , and where the allelic variant was present in at least 7

491 individuals of the ~30 samples (for each species). We retained those substitutions/indels
492 validated with the genome resequencing data. For this, of the genotype calls found in RNA
493 reads from brain/eyes of different stages, we kept only those that were also called in at least 8
494 of the 10 genome resequencing samples of each species. We considered this overlapping set
495 of variants as being fixed in *H. melpomene rosina* or *H. cydno chioneus*. Following a similar
496 approach to Bendesky *et al.*⁵⁹, we then restricted this set of substitutions between *cydno* and
497 *melpomene* to protein-coding regions, and selected those non-synonymous substitutions that
498 were considered to have moderate or high effect on protein function, with SNPeff⁷³. Finally,
499 we used the PROVEAN algorithm³³, to further study the functional effects of these
500 substitutions on protein function. The PROVEAN algorithm predicts the functional effect of
501 protein sequence variations based on how they affect alignments to homologous protein
502 sequences (for this we used the PROVEAN protein database online). We selected those amino
503 acid changes with the suggested PROVEAN score < -2.5, indicating non-neutral effect on
504 protein function.

505

506 **Admixture analyses.** We retrieved estimated admixture proportions between *H. melpomene*
507 *rosina* and *H. cydno chioneus*, for 100kb and 20kb windows, from Martin *et al.*³⁵

508

509 **Data accessibility.** RNA-seq data will be deposited on a public database

510 (<https://www.ebi.ac.uk/ena>) on acceptance. Analysis scripts and behavioural data are

511 available at: https://github.com/SpeciationBehaviour/neural_genes_heliconius.git

512

513 **Author contributions:** R.M.M. and M.R. conceived the study and designed the experiments,

514 with input from W.O.M. and C.D.J; M.R. analysed expression and sequence data; A.E.H.

515 analysed the behavioural data; T.J.T., S.H.M. and R.M.M. reared butterflies, dissected neural

516 tissue and extracted RNA; R.M.M., C.D.J. and W.O.M. secured funding, contributed

517 resources and provided supervision; R.P. additionally secured funding and contributed
518 resources; M.R. and R.M.M. wrote the manuscript with contributions from all authors.

519

520 **Acknowledgments**

521 We thank Liz Evans and Adriana Tapia for assistance in the insectaries. We are grateful to
522 Ana Pinharanda for sharing the *H. cydno* genome assembly and annotation and to Simon
523 Martin for sharing admixture proportions and comments on the manuscript. We thank the
524 Smithsonian Tropical Research Institute for providing research infrastructure, the Ministerio
525 del Ambiente for permission to collect butterflies in Panama, Edinburgh Genomics for
526 sequencing support and Jochen Wolf who kindly provided computational resources. MR,
527 AEH and RMM are supported by an Emmy Noether fellowship and research grant awarded to
528 RMM by the Deutsche Forschungsgemeinschaft (DFG) (Grant Number: GZ: ME 4845/1-1).
529 RMM was also supported by a Junior Research Fellowship from King’s College Cambridge,
530 an Ernst Mayr fellowship from the Smithsonian Tropical Research Institute, a Varley-
531 Gradwell fellowship from the Oxford University Museum of Natural History, and the
532 Balfour-Browne Fund, University of Cambridge. SHM was supported by a NERC IRF
533 (NE/N014936/1). This project was also supported by an Institutional Development Award
534 (IdeA) INBRE from the National Institute of General Medical Sciences (NIGMS) awarded to
535 RP (Grant number: P20GM103475), and a European Research Council (ERC) awarded to
536 CDJ (Grant number: 339873).

537

538 **References**

- 539 1. Coyne, J. A., Orr, H. A. *Speciation* (Sunderland, MA: Sinauer 2004).
- 540 2. Rosenthal, G. G. *Mate choice* (Princeton University Press, 2017).
- 541 3. Mayr, E. *Animal species and evolution* (Harvard University Press, 1963).
- 542 4. Cande, J., Prud’homme, B. & Gompel, N. Smells like evolution: The role of chemoreceptor
543 evolution in behavioural change. *Curr. Opin. Neurobiol.* **23**, 152–158 (2013).
- 544 5. Arguello, J. R. & Benton, R. Open questions: Tackling Darwin’s “instincts”: The genetic
545 basis of behavioural evolution. *BMC Biol.* **15**, 8–10 (2017).

- 546 6. Moehring, A. J. *et al.* Quantitative trait loci for sexual isolation between *Drosophila*
547 *simulans* and *D. mauritiana*. *Genetics* **167**, 1265–1274 (2004).
- 548 7. Shaw, K. L. & Lesnick S. C. Genomic linkage of male song and female acoustic preference
549 QTL underlying a rapid species radiation. *Proc. Natl. Acad. Sci. U. S. A.* **106**, 9737–9742
550 (2009).
- 551 8. Bay, R. A. *et al.* Genetic Coupling of Female Mate Choice with Polygenic Ecological
552 Divergence Facilitates Stickleback Speciation. *Curr. Biol.* **27**, 3344–3349 (2017).
- 553 9. Shahandeh, M. P., Pischedda, A., Rodriguez, J. M. & Turner, T. L. The genetics of male
554 pheromone preference difference between *Drosophila melanogaster* and *Drosophila*
555 *simulans*. *G3 Genes, Genomes, Genet.* **10**, 401–415 (2020).
- 556 10. Gould, F. *et al.* Sexual isolation of male moths explained by a single pheromone response
557 QTL containing four receptor genes. *Proc. Natl. Acad. Sci. U. S. A.* **107**, 8660–8665 (2010)
- 558 11. Leary, G. P. *et al.* Single mutation to a sex pheromone receptor provides adaptive specificity
559 between closely related moth species. *Proc. Natl. Acad. Sci. U. S. A.* **109**, 14081–14086
560 (2012).
- 561 12. Fan, P. *et al.* Genetic and neural mechanisms that inhibit *Drosophila* from mating with other
562 species. *Cell* **154**, 89–102 (2013).
- 563 13. Brand, P. *et al.* The evolution of sexual signaling is linked to odorant receptor tuning in
564 perfume-collecting orchid bees. *Nat. Commun.* **11** (2020).
- 565 14. Seehausen, O. *et al.* Speciation through sensory drive in cichlid fish. *Nature* **455**, 620–626
566 (2008).
- 567 15. Hench, K., Vargas, M., Höppner, M. P., McMillan, W. O. & Puebla, O. Inter-chromosomal
568 coupling between vision and pigmentation genes during genomic divergence. *Nat. Ecol.*
569 *Evol.* **3**, 657–667 (2019).
- 570 16. Merrill, R. M. *et al.* Disruptive ecological selection on a mating cue. *Proc. R. Soc. B Biol.*
571 *Sci.* **279**, 4907–4913 (2012).
- 572 17. Jiggins, C. D., Naisbit, R. E., Coe, R. L. & Mallet, J. Reproductive isolation caused by
573 colour pattern mimicry. *Nature* **411**, 302–305 (2001).
- 574 18. Jiggins, C. D. Ecological Speciation in Mimetic Butterflies. *Bioscience* **58**, 541–548 (2008).
- 575 19. Jiggins, C. D., Estrada, C. & Rodrigues, A. Mimicry and the evolution of premating
576 isolation in *Heliconius melpomene* Linnaeus. *J. Evol. Biol.* **17**, 680–691 (2004).
- 577 20. Merrill, R. M. *et al.* Genetic dissection of assortative mating behaviour. *PLoS Biol* **17**,
578 e2005902 (2018).
- 579 21. Reed, R. D. *et al.* Optix drives the repeated convergent evolution of butterfly wing pattern
580 mimicry. *Science* **333**, 1137–1141 (2011).
- 581 22. Martin, A. *et al.* Diversification of complex butterfly wing patterns by repeated regulatory
582 evolution of a Wnt ligand. *Proc. Natl. Acad. Sci. U. S. A.* **109**, 12632–12637 (2012).
- 583 23. Nadeau, N. J. *et al.* The gene cortex controls mimicry and crypsis in butterflies and moths.
584 *Nature* **534**, 106–110 (2016).
- 585 24. Felsenstein, J. Skepticism Towards Santa Rosalia, or Why Are There So Few Kinds of
586 Animals? *Evolution* **35**, 124–138 (1981).
- 587 25. Massey, J. H., Chung, D., Siwanowicz, I., Stern, D. L. & Wittkopp, P. J. The yellow gene
588 influences *Drosophila* male mating success through sex comb melanization. *Elife* **8**, 1–20
589 (2019).
- 590 26. Merrill, R. M., Van Schooten, B., Scott, J. A. & Jiggins, C. D. Pervasive genetic
591 associations between traits causing reproductive isolation in *Heliconius* butterflies. *Proc.*
592 *R. Soc. B Biol. Sci.* **278**, 511–518 (2011).
- 593 27. Seeholzer, L. F., Seppo, M., Stern, D. L. & Ruta, V. Evolution of a central neural circuit
594 underlies *Drosophila* mate preferences. *Nature* **559**, 564–569 (2018).
- 595 28. Martin, S. H. *et al.* Genome-wide evidence for speciation with gene flow in *Heliconius*
596 butterflies. *Genome Res.* **23**, 1817–1828 (2013).

- 597 29. Davey, J. *et al.* Major improvements to the *Heliconius melpomene* genome assembly used
598 to confirm 10 chromosome fusion events in 6 million years of butterfly evolution. *G3* **6**,
599 695–708 (2015).
- 600 30. Darragh, K. *et al.* A novel terpene synthase produces an anti-aphrodisiac pheromone in the
601 butterfly *Heliconius melpomene*. *bioRxiv*, 779678 (2019).
- 602 31. Wittkopp, P. J., Haerum, B. K. & Clark, A. G. Evolutionary changes in cis and trans gene
603 regulation. *Nature* **430**, 85–88 (2004).
- 604 32. Thomas, P. D. *et al.* Applications for protein sequence-function evolution data:
605 mRNA/protein expression analysis and coding SNP scoring tools. *Nucleic Acids Res.* **34**,
606 645–650 (2006).
- 607 33. Choi, Y., Sims, G. E., Murphy, S, Miller, J. R. & Chan, A. P. Predicting the Functional
608 Effect of Amino Acid Substitutions and Indels. *PLoS One* **7** (2012).
- 609 34. Martin, S. H., Davey, J. W. & Jiggins, C. D. Evaluating the use of ABBA-BABA statistics
610 to locate introgressed loci. *Mol. Biol. Evol.* **32**, 244–257 (2015).
- 611 35. Martin, S. H., Davey, J. W., Salazar, C. & Jiggins, C. D. Recombination rate variation
612 shapes barriers to introgression across butterfly genomes. *PLoS Biol.* **17**, 1–28 (2019).
- 613 36. Kopp, M. *et al.* Mechanisms of assortative mating in speciation with gene flow: Connecting
614 theory and empirical research. *Am. Nat.* **191**, 1–20 (2018).
- 615 37. Butlin, R. K. & Smadja, C. M. Coupling, reinforcement, and speciation. *Am. Nat.* **191**, 155–
616 172 (2018).
- 617 38. Westerman, E. L. *et al.* Aristaless controls butterfly wing color variation used in mimicry
618 and mate choice. *Current Biology*, **28**, 3469–3474 (2018).
- 619 39. Kronfrost, M. R. *et al.* Linkage of butterfly mate preference and wing color preference cue
620 at the genomic location of wingless. *Proc. Natl. Acad. Sci. U. S. A.* **103**, 6575–6580 (2006).
- 621 40. Chamberlain, N. L., Hill, R. I., Kapan, D. D., Gilbert, L. E., & Kronforst, M. R.
622 Polymorphic butterfly reveals the missing link in ecological speciation. *Science*, **326**, 847–
623 850 (2009).
- 624 41. McCulloch, K. J. *et al.* Sexual Dimorphism and Retinal Mosaic Diversification following
625 the Evolution of a Violet Receptor in Butterflies. *Mol. Biol. Evol.* **34**, 2271–2284 (2017).
- 626 42. Zaccardi, G., Kelber, A., Sison-Mangus, M. P. & Briscoe, A. D. Colour discrimination in
627 the red range with only one long-wavelength sensitive opsin. *J. Exp. Biol.* **209**, 1944–1955
628 (2006).
- 629 43. Monteiro, A. Gene regulatory networks reused to build novel traits. *BioEssays* **34**, 181–186
630 (2012).
- 631 44. Martin, A. *et al.* Multiple recent co-options of *Optix* associated with novel traits in adaptive
632 butterfly wing radiations. *Evodevo* **5** (2014).
- 633 45. Kandel, E. R, Schwartz, J. H., Jessell, T. M., Siegelbaum, S. A. & Hudspeth, A. J. *Principles*
634 *of Neural Science*, 2012th Ed. (New York: McGraw Hill, 2000).
- 635 46. Wang, X. *et al.* Genomic responses to selection for tame/aggressive behaviours in the silver
636 fox (*Vulpes vulpes*). *Proc. Natl. Acad. Sci. U. S. A.* **115**, 10398–10403 (2018).
- 637 47. Bloch, N. I. *et al.* Early neurogenomic response associated with variation in guppy female
638 mate preference. *Nat. Ecol. Evol.* **2**, 1772–1781 (2018).
- 639 48. Yamaguchi, M. Role of regucalcin in brain calcium signaling. *Integr. Biol.* **4**, 825–837
640 (2012).
- 641 49. Berridge, M. J. Neuronal calcium signaling. *Neuron*, **21**, 13–26 (1998).
- 642 50. Bashaw, G. J. & Klein, R. Signaling from axon guidance receptors. *Cold Spring Harb.*
643 *Perspect. Biol.* **2**, 1–17 (2010).
- 644 51. Prud'homme, B., Gompel, N. & Carroll, S. B. Emerging principles of regulatory
645 evolution. *Proc. Natl. Acad. Sci. U. S. A.* **104**, 8605–8612 (2007).
- 646 52. Preger-Ben Noon, E. *et al.* Comprehensive Analysis of a cis-Regulatory Region Reveals
647 Pleiotropy in Enhancer Function. *Cell Rep.* **22**, 3021–3031 (2018).

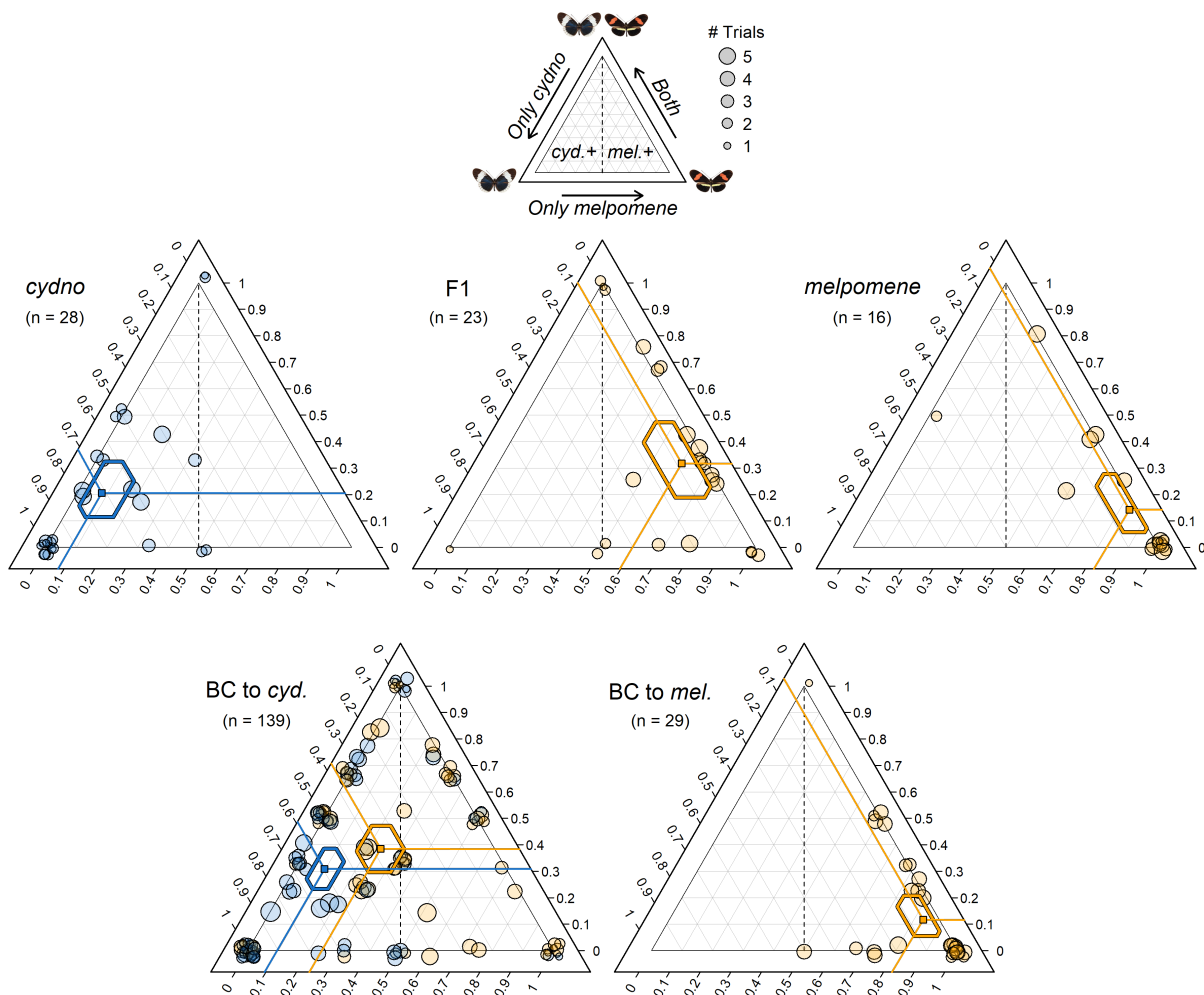
- 648 53. Lewis, J. *et al.* Parallel evolution of ancient, pleiotropic enhancers underlies butterfly wing
649 pattern mimicry. *Proc. Natl. Acad. Sci. U. S. A.* **116**, 24174–24183 (2019).
- 650 54. Zhang, W. *et al.* Comparative Transcriptomics Provides Insights into Reticulate and
651 Adaptive Evolution of a Butterfly Radiation. *Genome Biol. Evol.* **11**, 2963–2975 (2019).
- 652 55. Weber, J. N., Peterson, B. K. & Hoekstra, H. E. Discrete genetic modules are responsible
653 for complex burrow evolution in *Peromyscus* mice. *Nature* **493**, 402–405 (2013).
- 654 56. Cande, J., Andolfatto, P., Prud'homme, B., Stern, D. L. & Gompel, N. Evolution of Multiple
655 Additive Loci Caused Divergence between *Drosophila yakuba* and *D. santomea* in Wing
656 Rowing during Male Courtship. *PLoS One* **7**, 1–10 (2012).
- 657 57. McBride, C. S. *et al.* Evolution of mosquito preference for humans linked to an odorant
658 receptor. *Nature* **515**, 222–227 (2014).
- 659 58. Ding, Y., Berrocal, A., Morita, T., Longden, K. D. & Stern, D. L. Natural courtship song
660 variation caused by an intronic retroelement in an ion channel gene. *Nature* **536**, 329–332
661 (2016).
- 662 59. Bendesky, A. *et al.* The genetic basis of parental care evolution in monogamous mice.
663 *Nature* **544**, 434–439 (2017).
- 664 60. Auer, T. O. *et al.* Olfactory receptor and circuit evolution promote host
665 specialization. *Nature*, 1–7 (2020).
- 666 61. Vehtari, A., Gelman, A. & Gabry, J. Practical Bayesian model evaluation using leave-one-
667 out cross-validation and WAIC. *Stat. Comput.* **27**, 1413–1432 (2017).
- 668 62. Jiggins, C. D. *The ecology and evolution of Heliconius butterflies* (Oxford University Press,
669 2016).
- 670 63. Pinharanda, A. *et al.* Sexually dimorphic gene expression and transcriptome evolution
671 provide mixed evidence for a fast-Z effect in *Heliconius*. *J. Evol. Biol.* **32**, 194–204 (2019).
- 672 64. Dobin, A. *et al.* STAR: Ultrafast universal RNA-seq aligner. *Bioinformatics* **29**, 15–21
673 (2013).
- 674 65. Li, H. *et al.* The Sequence Alignment/Map format and SAMtools. *Bioinformatics* **25**, 2078–
675 2079 (2009).
- 676 66. Anders, S., Pyl, P. T. & Huber, W. HTSeq-A Python framework to work with high-
677 throughput sequencing data. *Bioinformatics* **31**, 166–169 (2015).
- 678 67. Love, M. I. Huber, W. & Anders, S. Moderated estimation of fold change and dispersion
679 for RNA-seq data with DESeq2. *Genome Biol.* **15**, 1–21 (2014).
- 680 68. Montgomery, S. H. & Mank, J. E. Inferring regulatory change from gene expression: the
681 confounding effects of tissue scaling. *Mol. Ecol.* **25**, 5114–5128 (2016).
- 682 69. McKenna, A. *et al.* The genome analysis toolkit: A MapReduce framework for analyzing
683 next-generation DNA sequencing data. *Genome Res.* **20**, 1297–1303 (2010).
- 684 70. Finn, R. D. *et al.* InterPro in 2017-beyond protein family and domain annotations. *Nucleic
685 Acids Res.* **45**, D190–D199 (2017).
- 686 71. Roberts, A., Pimentel, H., Trapnell, C. & Pachter, L. Identification of novel transcripts in
687 annotated genomes using RNA-seq. *Bioinformatics* **27**, 2325–2329 (2011).
- 688 72. York, R. A. *et al.* Behaviour-dependent cis regulation reveals genes and pathways
689 associated with bower building in cichlid fishes. *Proc. Natl. Acad. Sci. U. S. A.* **115**, 1081–
690 1090 (2018).
- 691 73. Cingolani, P. *et al.* A program for annotating and predicting the effects of single nucleotide
692 polymorphisms, SnpEff *Fly*. **6**, 80–92 (2012).

693
694
695
696

697

Figures

698 **Figure 1. Genotype at the preference QTL on chromosome 18 influences courtship**
 699 **initiation.** Ternary plots showing the number of 15-minute choice trials in which courtship was
 700 initiated towards *melpomene*, *cydno* or both females for different male types. Left ternary axis
 701 shows proportion of trials where courtship was initiated towards *H. cydno* female only, bottom
 702 axis towards *H. melpomene* female only, and right axis towards both female species. Orange
 703 points represent individuals that have inherited at least one *melpomene* derived allele at the
 704 preference QTL on chromosome 18 (i.e. either *melp/melp* or *cyd/melp*); and blue points
 705 represent individuals that are homozygous for *cydno* alleles at the preference QTL on
 706 chromosome 18 (i.e. *cyd/cyd*). Point size is scaled to the number of trials in which the male
 707 showed a response and a ‘jitter’ function has been applied. 95% credibility intervals (CrIs) for
 708 all three proportions are shown as hexagons around predictors with lines projecting to
 709 corresponding values on the three axes.
 710



711

712

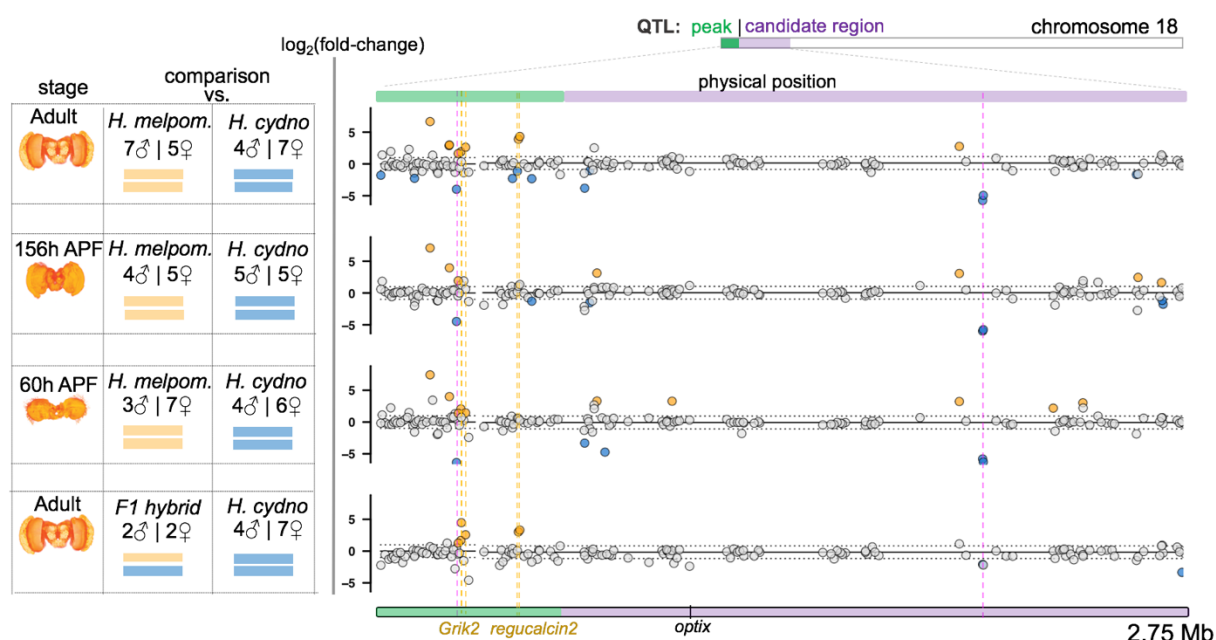
713

714

715

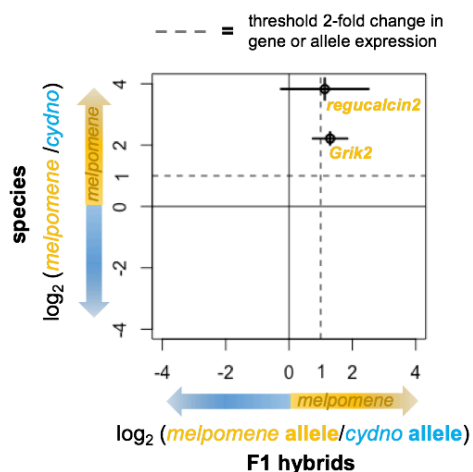
716

717 **Figure 2. Differential expression at the preference QTL region on chromosome 18.** Left:
 718 Summary of the comparative transcriptomic analyses with stage, number of samples and
 719 chromosome 18 composition. Right: the corresponding results, zooming in on the QTL region
 720 on chromosome 18. The *x*-axis represents physical position. The QTL peak, and the rest of the
 721 QTL 1.5 LOD candidate region (from²⁸) are shown in green and purple, respectively. Points
 722 correspond to individual genes, with the *y*-axis indicating the $\log_2(\text{fold-change})$ for each
 723 comparison. The two horizontal dashed lines (at *y*-values of 1 and -1) indicate a 2-fold change
 724 in expression. Genes showing a significant 2-fold+ change in expression level between groups
 725 are highlighted in orange and blue, where orange indicates higher levels in *melpomene* or in the
 726 hybrids *cyd/melp* (blue if in *cydno* – hybrids *cyd/cyd*). Vertical dashed lines highlight those
 727 genes that are differentially expressed between *melpomene* and *cydno* AND between *cyd/melp*
 728 vs *cyd/cyd* individuals, at the same stage. Two genes highlighted by dashed fuchsia vertical
 729 lines were excluded because they did not show differential expression, or showed reversal of
 730 the fold change when mapping RNA-seq reads to the *H. cydno* genome. Note that *Heliconius*
 731 brain (reconstruction) images, added for reference, do not include the eyes (ommatidia and
 732 retinal membrane).
 733

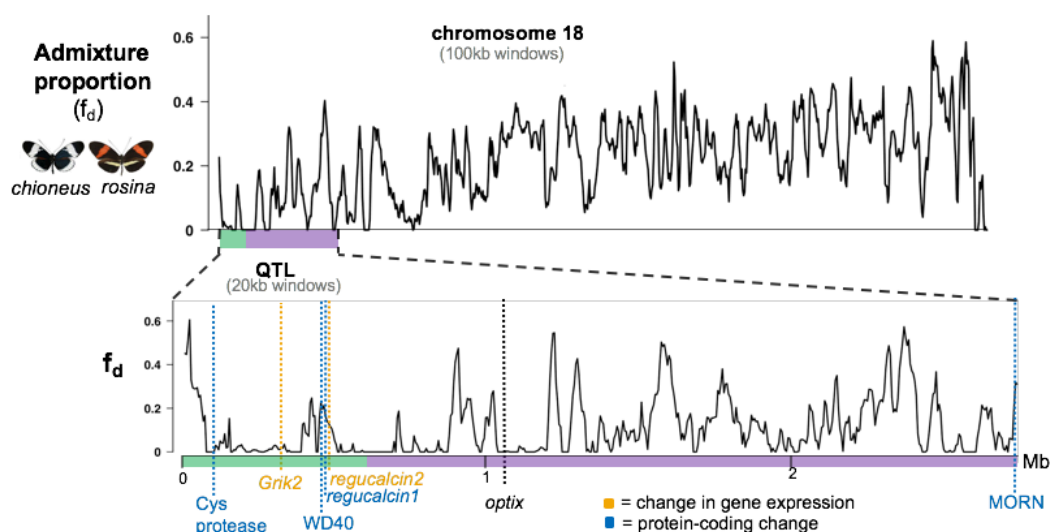


734
 735
 736
 737
 738
 739
 740
 741
 742
 743

744 **Figure 3. *Grik2* and *Regucalcin2* show evidence of allele specific expression.** Points indicate
 745 the value, and bars the standard error, of the (base 2) logarithmic fold change in expression
 746 between parental species (horizontal) and the alleles in F1 hybrids (vertical), for candidate
 747 genes (as defined in the transcript-guided annotation). Dashed lines indicate the threshold for a
 748 2-fold change in expression for the genes in the species (horizontal), and for the alleles in the
 749 hybrids (vertical).
 750



751
 752
 753
 754 **Figure 4. Gene flow at the QTL region for behaviour.** Admixture proportion (f_d) values
 755 estimated in overlapping 100kb (top) and 20kb (bottom) windows for chromosome 18 (top) and
 756 the QTL region (bottom) between *H. melpomene rosina* and *H. cydno chioneus*, with candidate
 757 genes positions highlighted by a vertical dashed line, and *optix* location displayed for reference.
 758 The x-axis represents physical position, the y-axis indicates the f_d value. f_d values close to zero
 759 indicate that the proportion of shared derived alleles, and consequently gene flow, between
 760 *melpomene* and *cydno* is small (or zero), implying localized selection against foreign alleles
 761 that introgress between the two species.
 762



763
 764

1 **Supplementary information: Visual mate preference evolution**
2 **during butterfly speciation is linked to neural processing genes**

3
4 Matteo Rossi^{1,2}, Alexander E. Hausmann¹, Timothy J. Thurman^{2,3}, Stephen H. Montgomery⁴,
5 Riccardo Papa^{2,5,6}, Chris D. Jiggins⁷, W. Owen McMillan² & Richard M. Merrill^{1,2*}

6
7 *1. Division of Evolutionary Biology, LMU, Munich, Germany; 2. Smithsonian Tropical Research Institute,*
8 *Panama City, Panama; 3. Division of Biological Sciences, University of Montana, USA; 4. School of Biological*
9 *Sciences, University of Bristol, Bristol, UK; 5. Department of Biology, University of Puerto Rico, San Juan,*
10 *Puerto Rico; 6. Molecular Sciences and Research Center, University of Puerto Rico, San Juan, Puerto Rico;*
11 *7. Department of Zoology, University of Cambridge, Cambridge UK. *corresponding author:*
12 merrill@bio.lmu.de
13
14
15
16
17
18
19
20
21
22
23
24
25
26
27
28
29
30
31
32
33
34
35
36
37
38

39
40
41
42
43
44
45
46
47
48
49
50
51
52
53
54
55
56
57
58
59
60
61
62
63
64
65

Supplementary methods and results

Mapping RNA-seq reads to the *Heliconius cydno* genome. To determine whether the *H. melpomene* reference genome introduced mapping biases of RNA-seq reads, possibly affecting differential expression estimates, we also mapped to a *H. cydno* assembly/annotation. Generally, we found similar patterns of differential expression when mapping to the two genomes. Since **i)** we observed an equal decrease (~ 40 %) of genes showing 2-fold changes in *melpomene* and *cydno* when mapping to *H. cydno*, at every stage (p-value=0.317 at adult stage, p-value=0.800 at 156h APF, p-value=0.897 at 60h APFP, Fisher's Exact test, **Table S2**), and **ii)** this decrease was widespread throughout the genome, we concluded that the *melpomene* reference genome did not bias differential gene expression analyses.

Allele-specific expression in the introgression line. BC3 hybrids had different combinations of chromosomes segregating for the *melpomene* alleles in a *cydno* background. Therefore, in principle, we could not infer *cis-* or *trans-* gene regulatory effects genome-wide from the profiles of allele specific expression (ASE) in these hybrids as for F1 hybrids, due to the diverse trans-acting environments. However, previous analyses (comparing gene expression levels between hybrids carrying *cyd/melp* vs. *cyd/cyd* regions on chromosomes other than 18) imply that differential expression of the candidate genes seems to be driven by the *melpomene* copy difference within the introgressed region on chromosome 18. Therefore, ASE analyses of candidate genes in BC3 hybrids carrying *cyd/melp* alleles on chromosome 18 should indicate whether the differences are due to *cis-* or *trans-*regulatory effects from within the introgressed region (**Figure S6**).

66 In BC3 hybrids sampled at 156h APF and 60hAPF, the *melpomene* and *cydno* alleles of the
67 *ionotropic glutamate receptor (Grik2)* are expressed at very similar levels (at 156hAPF p
68 value=0.841, at 60hAPF p value=0.579, Wald test), suggesting trans-only regulatory effects at
69 these stages for *Grik2*. For *regucalcin1* we again had very few allele-informative read counts
70 in hybrids at 156h APF. Although there was a tendency towards up regulation of the
71 *melpomene* allele, there was no statistical significance to support this (p=0.174, Wald test).
72 We detected diffASE expression of *regucalcin2* only at 60h APF (p <0.001, Wald test), but at
73 this stage *regucalcin2* was not detected as differentially expressed between pure species.
74 Thus, although there is tentative evidence for *cis*-regulatory effects for species differences in
75 *regucalcin* expression during development, it is not conclusive.

76

77

78

79

80

81

82

83

84

85

86

87

88

89

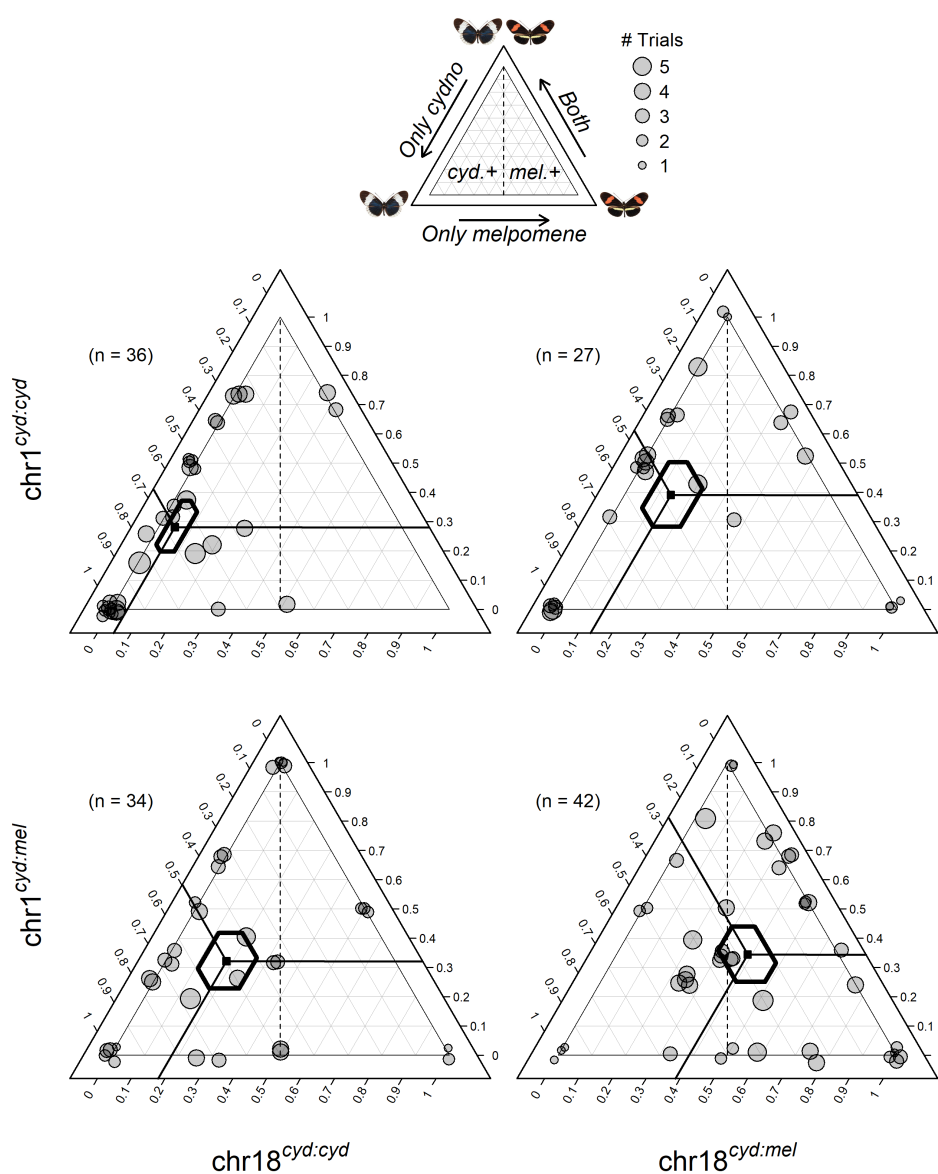
90

91

92
93
94
95
96
97
98
99
100
101
102
103
104
105

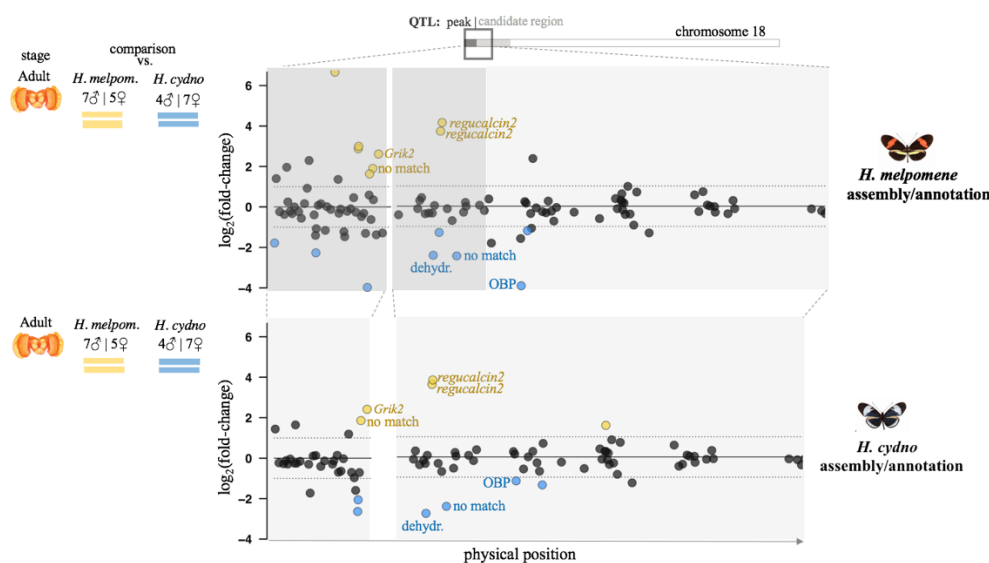
Supplementary figures

Figure S1. Ternary plots showing the number of 15-minute choice trials in which courtship was initiated towards *melpomene*, *cydno* or both females for backcross-to-*cydno* males, with different genotypes at the two QTLs retained in our model (on chromosome 1 and chromosome 18). Left ternary axis shows proportion of trials where courtship was initiated towards *H. cydno* female only, bottom axis towards *H. melpomene* female only, and right axis towards both female species. Each point corresponds to a male (and a ‘jitter’ function applied). Point size is scaled to the number of trials in which the male showed a response. 95% credibility intervals (CrIs) for all three proportions are shown as hexagons around predictors extrapolated from the statistical model with the best fit, with lines projecting to corresponding values on the three axes.



106
107

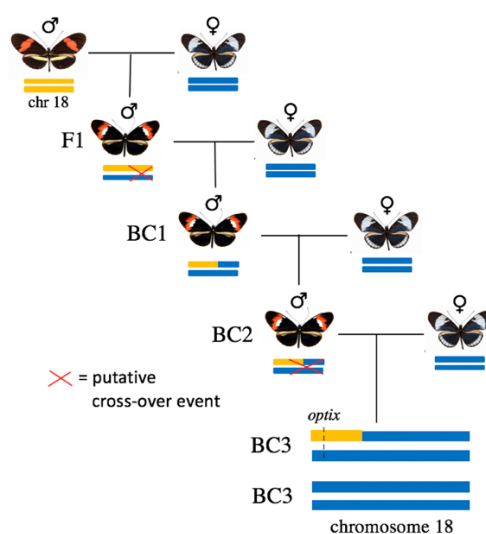
108 **Figure S2.** Results of comparative transcriptomic analyses between *melpomene* and *cydno* (in
 109 the imago) when mapping RNA-seq reads to the *H. melpomene* assembly/annotation (top), and
 110 to the *H. cydno* assembly/annotation (bottom), zooming in on the QTL region on chromosome
 111 18. The x-axis represents physical position. Points correspond to individual genes, with the y-
 112 axis indicating the $\log_2(\text{fold-change})$ for each comparison. The two horizontal dashed lines (at
 113 y-values of 1 and -1) indicate a 2-fold change in expression. Genes showing a significant 2-
 114 fold+ change in expression level between groups are highlighted in orange and blue, where
 115 orange indicates higher levels in *melpomene*, blue if in *cydno*. Genes detected as differentially
 116 expressed mapping to both *melpomene* and *cydno* genomes are labelled with gene names.
 117 dehydr.=2-oxoisovalerate dehydrogenase, OBP=odorant-binding protein.
 118



119
 120

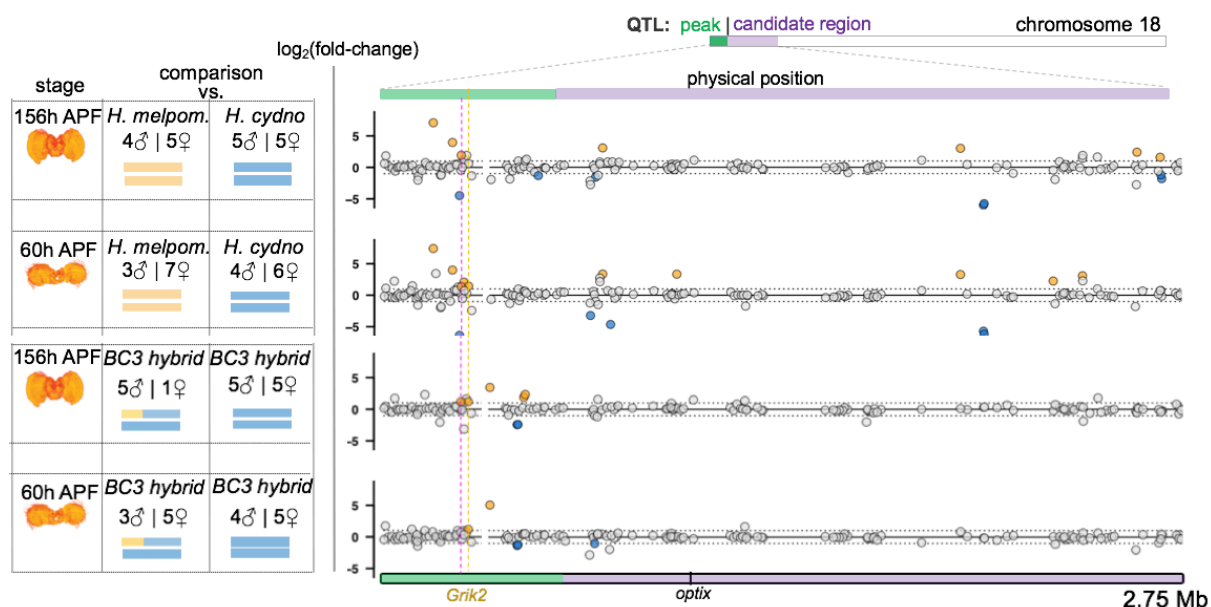
121
 122
 123
 124
 125
 126
 127
 128
 129
 130
 131
 132
 133
 134
 135
 136
 137
 138

139 **Figure S3.** Crossing design for producing backcross hybrids segregating at the QTL on
140 chromosome 18. This introgression line was created by outcrossing a male hybrid to *H. cydno*
141 females over three generations, selecting a hybrid male that showed a red band on the wing at
142 each generation. This meant that these males carried one copy of the *H. melpomene* allele at the
143 *optix* locus. We expected that, following recombination (which occurs in males), by the fourth
144 generation we would remain with two types of individuals: either *cyd/melp* or *cyd/cyd* at the
145 level of the *optix* region (which approximately corresponds to the region associated with male
146 preference behaviour).
147
148



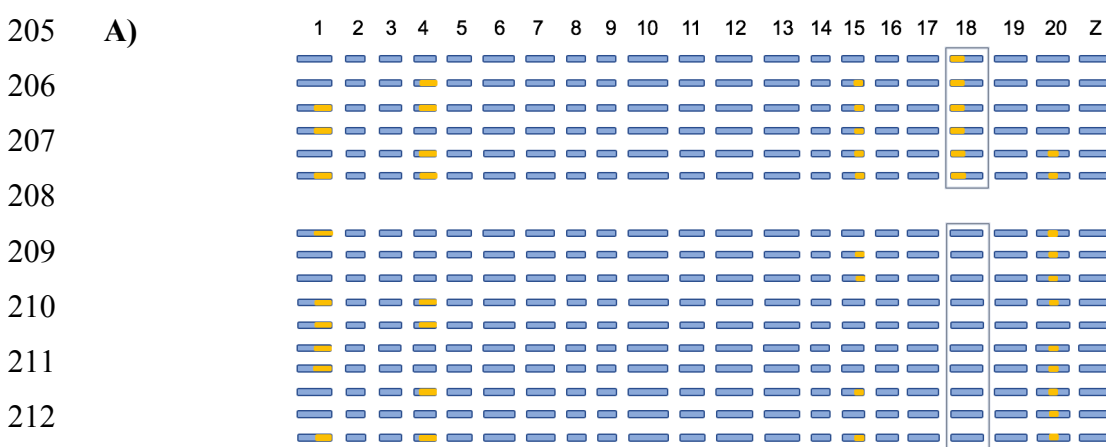
149
150
151
152
153
154
155
156
157
158
159
160
161
162
163
164
165

166 **Figure S4.** Differential gene expression at the QTL region at pupal stages. Left: summary of
 167 the comparative transcriptomic analyses with stage, number of samples and chromosome 18
 168 composition. Right: the corresponding results, zooming in on the QTL region on chromosome
 169 18. The x-axis represents physical position. The QTL peak, and the rest of the QTL 1.5 LOD
 170 candidate region are shown in green and purple, respectively. Points correspond to individual
 171 genes, with the y-axis indicating the $\log_2(\text{fold-change})$ for each comparison. The two horizontal
 172 dashed lines (at y-values of 1 and -1) indicate a 2-fold change in expression. Genes showing a
 173 significant 2-fold+ change in expression level between groups are highlighted in orange and
 174 blue, where orange indicates higher levels in *melpomene* or in the hybrids *cyd/melp* (blue if in
 175 *cydno* – hybrids *cyd/cyd*). Vertical dashed lines highlight those genes that are differentially
 176 expressed between *melpomene* and *cydno* AND between *cyd/melp* vs *cyd/cyd* individuals, at
 177 the same stage. One gene highlighted by a dashed fuchsia vertical line was excluded because it
 178 showed reversal of the fold change when mapping RNA-seq reads to the *H. cydno* genome.
 179

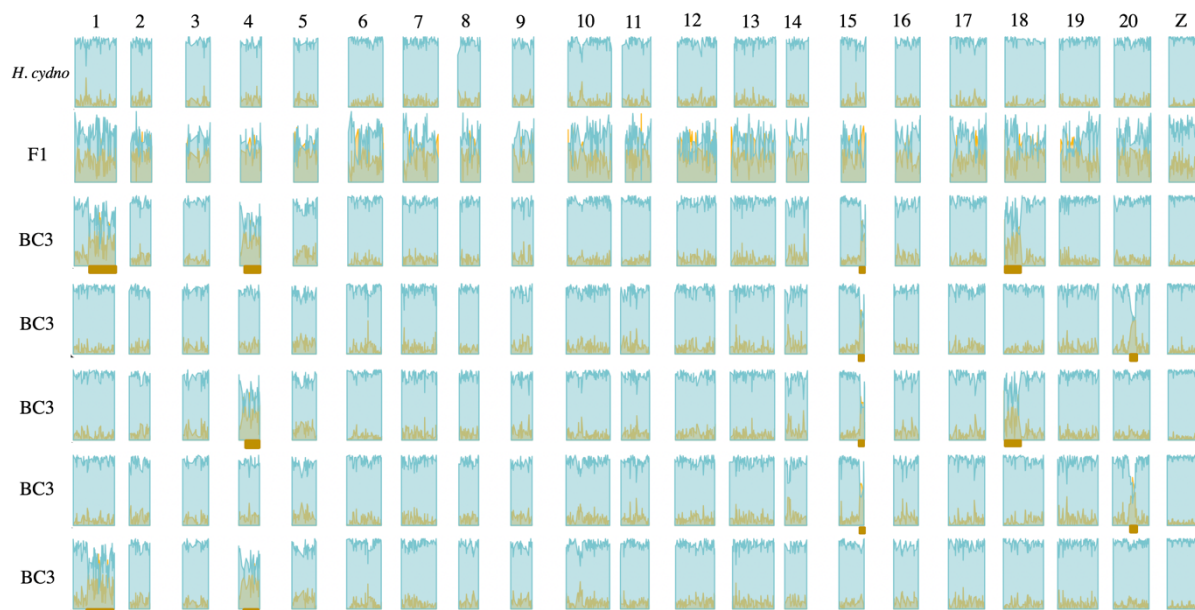
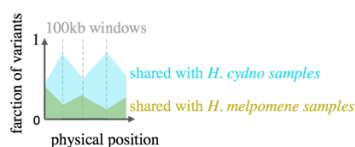


180
 181
 182
 183
 184
 185
 186
 187
 188
 189
 190
 191
 192

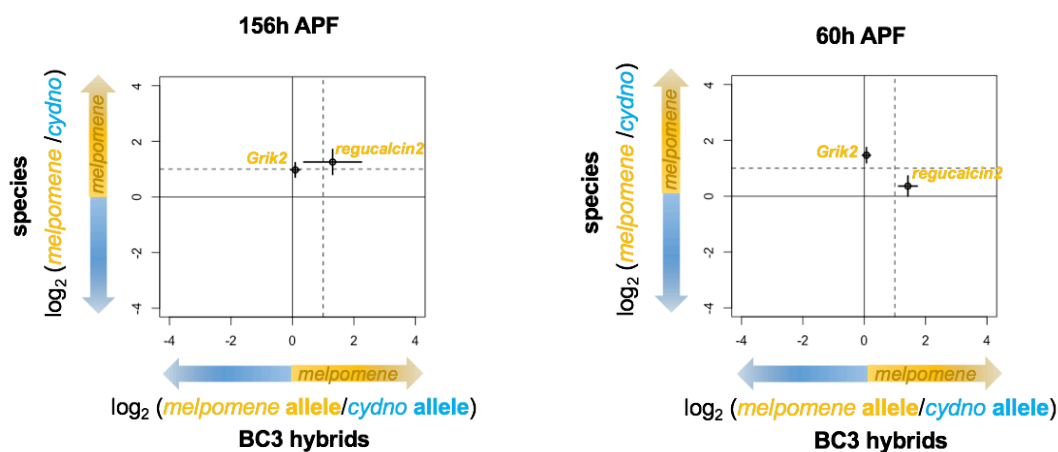
193 **Figure S5. A)** Schematic representation of hybrid pupae (sampled at 156h APF) genome
 194 composition. Columns represent chromosomes, rows represent individuals, orange indicates
 195 *cyd/melp* regions, blue indicates *cyd/cyd* regions. **B)** Genome composition of (a subset of) BC3
 196 hybrids. We calculated the fraction of SNPs and indels that each BC3 hybrid, one *cydno* and
 197 one F1 hybrid samples shared with *melpomene* and *cydno* samples, in non-overlapping 100kb
 198 windows. x-axes represent physical position (for each chromosome), y-axes fractions of shared
 199 variants with *melpomene* (in gold) and with *cydno* (in light blue). Matching variant fractions
 200 between BC3 hybrids and the F1 hybrid, indicating heterozygous regions, are highlighted with
 201 a gold bar underneath. Note that the general trend of higher number of variants shared with *H.*
 202 *cydno* in heterozygous regions is due to the fact that we inferred variants by mapping to the *H.*
 203 *melpomene* genome (and used variant sites only for this analysis).



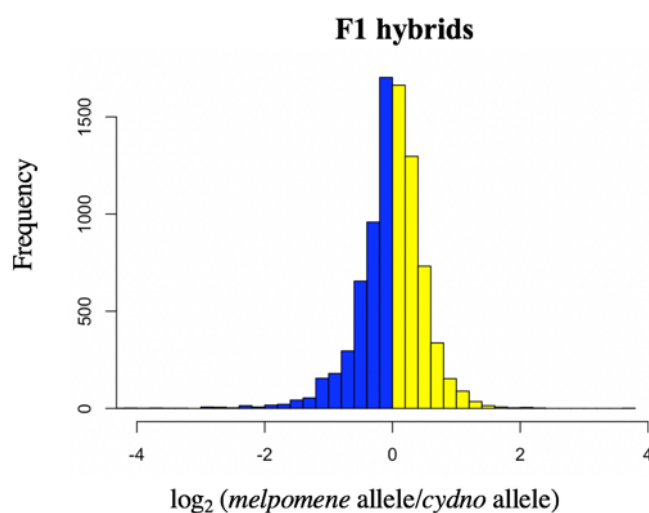
214 **B)**



217 **Figure S6.** Allele specific expression profiles of candidate genes at pupal stages. Points indicate
 218 the value, and bars the standard error, of the (base 2) logarithmic fold change in expression
 219 between parental species (horizontal) and the alleles in F1 hybrids (vertical), for candidate
 220 genes (as defined in the transcript-guided annotation). Dashed lines indicate the threshold for a
 221 2-fold change in expression for the genes in the species (horizontal), and for the alleles in the
 222 hybrids (vertical).
 223
 224



225
 226
 227 **Figure S7.** Distribution of the (base 2) logarithmic fold change in allele expression. Coloured
 228 bars indicate the number of genes showing a bias in expression for the *cydrno* allele (in blue)
 229 and for the *melpomene* allele (in yellow). Values departing from 0 on the x-axis, indicate an
 230 increase in the fold change for the *cydrno* allele (negative values) or for the *melpomene* allele
 231 (positive values), respectively.
 232



233
 234
 235
 236
 237

238
239
240
241
242
243
244
245

Supplementary tables

Table S1. List of differentially expressed genes in species and hybrids comparisons.

A) QTL chromosome 1. Orange indicates genes up-regulated in *H. melpomene*, and blue those up-regulated in *H. cydno*.

#	Gene name (Hmel2.5)	Annotated function	Species comparison		
			60h APF	156h APF	Imago
1	HMEL002973g1	No match	✓	✓	✓
2	HMEL003796g1	Regulation of enolase protein 1	✓	✗	✓
3	HMEL011272g1	no match	✗	✓	✓
4	HMEL030024g1	Ribonuclease H superfamily	✓	✓	✓
5	HMEL030042g1	SWR1-complex protein 5	✗	✗	✓
6	HMEL030052g1	reverse transcriptase	✓	✓	✓
7	HMEL005260g1	unknown	✗	✓	✗
8	HMEL030040g1	No match	✗	✓	✗
9	HMEL030037g1	No match	✓	✓	✗
10	HMEL010076g1	Amino acid transporter	✓	✗	✗

246
247
248
249
250
251
252
253
254
255
256
257
258
259
260
261
262
263
264
265
266
267
268
269
270
271

272 **B) QTL chromosome 18.** Those genes found to be differentially expressed when also mapping
 273 to the *H. cydno* genome are highlighted in bold. Genes annotated as distinct but sharing the
 274 same number in the table (#) were later found to be single genes (see second paragraph of the
 275 Results section).
 276
 277

#	Gene name (Hmel2.5)	Annotated function	Species comparison			Hybrids comparison		
			60h APF	156h APF	Imag o	60h APF	156h APF	Imag o
1	HMEL009992g1	No match	✓	✗	✓	✗	✗	✓
1	HMEL009992g4	<i>Ionotropic glutamate receptor</i>	✓	✗	✓	✓	✓	✓
2	HMEL009996g1	<i>Gag-related protein</i>	✓	✓	✓	✗	✗	✗
3	HMEL034168g1	unknown	✗	✗	✓	✗	✗	✗
4	HMEL034173g1	<i>SWR1-complex protein 5</i>	✗	✗	✓	✗	✗	✗
5	HMEL034176g1	<i>Aspartic peptidase</i>	✓	✓	✓	✗	✗	✗
6	HMEL034184g1	No match	✗	✗	✓	✗	✗	✗
7	HMEL034185g1	No match	✓	✓	✓	✗	✗	✗
8	HMEL034187g1	<i>Major facilitator superfamily (MFS) transporter</i>	✓	✓	✓	✗	✓	✓
9	HMEL003176	<i>Odorant binding protein</i>	✗	✓	✓	✓	✗	✗
10	HMEL013551g1	<i>2-oxoisovalerate dehydrogenase</i>	✗	✗	✗	✓	✓	✗
10	HMEL013551g2	<i>2-oxoisovalerate dehydrogenase</i>	✗	✗	✓	✓	✗	✗
11	HMEL013551g4	<i>SMP-30/regucalcin</i>	✗	✗	✓	✗	✗	✗
12	HMEL013552g1	<i>SMP-30/regucalcin</i>	✗	✗	✓	✗	✓	✓
12	HMEL034199g1	<i>SMP-30/regucalcin</i>	✗	✗	✓	✗	✓	✓
13	HMEL014202g1	<i>Catalase</i>	✗	✗	✓	✗	✗	✗
14	HMEL014202g3	<i>Catalase</i>	✗	✓	✗	✗	✗	✗
15	HMEL034201g1	No match	✗	✗	✓	✗	✗	✗
16	HMEL034205g1	No match	✓	✗	✓	✗	✗	✗
17	HMEL034227g1	<i>Ribonuclease H superfamily</i>	✓	✓	✓	✗	✗	✗
18	HMEL034229g1	<i>Endonuclease/exonuclease/phosphatase superfamily</i>	✓	✓	✓	✗	✗	✓
19	HMEL034230g1	No match	✓	✓	✓	✗	✗	✗
20	HMEL003863g1	<i>Vacuolar protein sorting-associated (VPS) protein</i>	✓	✓	✗	✗	✗	✗
21	HMEL003863g3	No match	✓	✗	✗	✗	✗	✗
22	HMEL006662g1	<i>Serpin family protein</i>	✗	✓	✗	✗	✗	✗
23	HMEL006663	<i>Odorant binding protein</i>	✗	✓	✗	✗	✗	✗
24	HMEL022553	<i>Odorant binding protein</i>	✗	✓	✗	✗	✗	✗
25	HMEL001038g1	<i>Monocarboxylate transporter</i>	✓	✗	✗	✗	✗	✗
26	HMEL014190g1	unknown function	✓	✗	✗	✗	✗	✗
27	HMEL034236g1	No match	✓	✗	✗	✗	✗	✗
28	HMEL034189g1	<i>PiggyBac transposable element-derived protein</i>	✗	✗	✗	✗	✗	✓
29	HMEL034246g1	No match	✗	✗	✗	✗	✗	✓
30	HMEL034195g1	<i>Gag-related protein</i>	✗	✗	✗	✓	✓	✗

278 **Table S2.** Number of genes showing significant >2-fold change in expression, at different
279 stages, mapping to the *melpomene* and to the *cydno* genomes. Note that the considerable
280 reduction in the number of genes detected as differentially expressed when mapping to *H. cydno*
281 is most likely a result of the lower quality/completeness of the *H. cydno* genome assembly.
282

Stage	Mapping to:	Up-regulated in <i>H. melpomene</i>	Up-regulated in <i>H. cydno</i>
Adult	<i>H. melpomene</i>	694	733
	<i>H. cydno</i>	390	451
156h APF	<i>H. melpomene</i>	837	667
	<i>H. cydno</i>	518	403
60h APF	<i>H. melpomene</i>	846	642
	<i>H. cydno</i>	490	376

283
284
285
286
287
288
289
290
291
292
293
294
295
296
297
298
299
300
301
302
303
304
305
306
307
308
309
310
311

312 **Table S3.** Heterozygosity on the Z-chromosome. Heterozygosity is calculated as proportion of
 313 variants (SNPs and indels) which are heterozygous, in each sample, rounded at the second
 314 decimal place (note that variant sites were inferred having mapped to the *H. melpomene*
 315 genome).
 316

<i>H. melpomene</i>				<i>H. cydno</i>			
Males		Females		Males		Females	
ID	Het.	ID	Het.	ID	Het.	ID	Het.
Adults							
45	0.49	53	0.04	57	0.23	50	0.02
47	0.46	78	0.05	82	0.23	51	0.02
70	0.47	80	0.04	98	0.25	58	0.02
71	0.48	128	0.04	99	0.24	67	0.02
83	0.46	218	0.05			68	0.01
100	0.49					81	0.02
104	0.46					84	0.02
156h APF							
5	0.47	6	0.05	4	0.26	13	0.02
14	0.49	18	0.05	8	0.26	21	0.04
17	0.49	24	0.05	142	0.30	30	0.03
184	0.50	150	0.05	151	0.29	137	0.04
		220	0.06	156	0.29	168	0.04
60h APF							
92	0.48	87	0.06	85	0.26	90	0.02
97	0.49	95	0.05	86	0.27	118	0.02
115	0.47	117	0.05	119	0.27	125	0.02
		124	0.04	146	0.26	144	0.02
		149	0.06			162	0.02
		164	0.05			200	0.02
		208	0.06				

317

Hybrids							
Males		Females		Males		Females	
ID	Het.	ID	Het.	ID	Het.	ID	Het.
F1 hybrids (adults)							
42	0.64	56	0.05				
49	0.64	69	0.04				
Introgression line -156h APF				Introgression line – 60h APF			
105	0.26	108	0.02	152	0.27	161	0.02
116	0.27	123	0.02	193	0.27	165	0.02
126	0.27	136	0.02	198	0.25	179	0.02
131	0.27	139	0.02	199	0.27	187	0.02
133	0.26	140	0.02	201	0.26	188	0.02
154	0.26	166	0.02	212	0.28	192	0.02
155	0.26			215	0.27	197	0.02
183	0.27					209	0.03
185	0.27					214	0.02
189	0.27					224	0.02

318

319

320